

Original Article

Electron Beam Dose Distribution in the Presence of Non-Uniform Magnetic Field

Mohamad Javad Tahmasebi-Birgani¹, Mohamad Reza Bayatiani^{2*}, Fatemeh Seif², Mansur Zabihzadeh¹, Hojatolah Shahbazian¹

Abstract

Introduction

Magnetic fields are capable of altering the trajectory of electron beams and can be used in radiation therapy. The aim of this study was to produce regions with dose enhancement and reduction in the medium.

Materials and Methods

The NdFeB permanent magnets were arranged on the electron applicator in several configurations. Then, after the passage of the electron beams (9 and 15 MeV Varian 2100C/D) through the non-uniform magnetic field, the Percentage Depth Dose (PDDs) on central axis and dose profiles in three depths for each energy were measured in a 3D water phantom.

Results

For all magnet arrangements and for two different energies, the surface dose increment and shift in depth of maximum dose (d_{max}) were observed. In addition, the pattern of dose distribution in buildup region was changed. Measurement of dose profile showed dose localization and spreading in some other regions.

Conclusion

The results of this study confirm that using magnetic field can alter the dose deposition patterns and as a result can produce dose enhancement as well as dose reduction in the medium using high-energy electron beams. These effects provide dose distribution with arbitrary shapes for use in radiation therapy.

Keywords: Electron Beam; Magnetic Field; Radiation Therapy.

1- Department of Medical Physics, Jundishapur University of Medical Sciences, Ahvaz, Iran

2- Radiotherapy and Medical Physics Department of Arak University of Medical Sciences & Khansari Hospital, Arak, Iran

*Corresponding Author: Tel: +989166009472; E-Mail: bayatiani@arakmu.ac.ir

1. Introduction

In the absence of electric field, the force (F) on a moving electron with velocity (v) and charge (e) in a magnetic field (B) becomes [1]:

$$F = m \frac{dv}{dt} = ev \times B \quad (1)$$

In the situation where the magnetic field is in the Z axis (parallel to central axis of electron beam), the Z component of the velocity along the magnetic field is not affected, but the X and Y components of the velocity vector vary as [2]:

$$\frac{dv_x}{dt} = \left(\frac{e}{m}\right) B_z v_y \quad \text{And} \quad \frac{dv_y}{dt} = \left(\frac{e}{m}\right) B_z v_x \quad (3)$$

This equation shows the electrons that normally would have been released their energy in the off-axis, in the absence of the magnetic field enter to the region near the central axis. In the other hand, studying ionizing radiation on biological systems shows that radiation exposures induce biological damage in DNA of cells. Successful cell killing occurs when a sufficient number of breaks in DNA occur within close proximity [3, 4]. This begs the question of whether magnetic field can be used to alter the path of charged particles (electrons in this research) in such a way to focus them on tumors as a target in electron radiation therapy. Evaluation of the effect of magnetic field on dose distribution has been studied for along time. Bostike was the first person who proposed that the dose distribution can be improve by placing the media in magnetic field [5].

The electron beams enter the transverse magnetic field following a spiral motion that tends to reduce the velocity of the electrons. The results of this process are to increase the maximum dose and change the location of buildup region and skin sparing as a result of the reduction in the surface dose [6-8]. Some researchers have shown that the dose deposition can be forced by the transverse magnetic field to follow a rapid drop-off [9, 10]. This field can be used to increase the dose to the tumor and reduce the dose to adjacent normal tissues. The enhancement of dose refer to the

trapping of electrons in a specific area and the dose reduction is due to the loss of transient charged particle equilibrium downstream from the magnetic field [11, 12].

Some studies suggest that the magnetic field can be used in conjunction with electron therapy and demonstrated that lateral spread of 10 and 20 MeV could be reduced from many centimeters to a few millimeters. These magnetic fields, due to the lateral confinement of the electron trajectories in the phantom, can be used to reduce the undesirable effects caused by loss in charged particle equilibrium (CPE) near air cavities [13, 14].

Although the magnetic field has a direct effect on the dose deposition patterns of electron beams, dosimetric properties of photon beams can be modified by applying the magnetic field. Because of the influence of secondary electrons, the magnetic field can significantly reduce the lateral spread of scattered and secondary electrons that will lead to a change in the penumbra for photon beam irradiation [15]. The main issue in the magnetic field, conjunction with photon beam, is that the magnetic field cannot directly affect the photon beam. For this reason, the magnetic field must be applied to the phantom and in these circumstances; the magnetic poles are far away from each other. To compensate this loss, a high-intensity magnetic field should be used but consequently the magnet weight will go up and the cost would be prohibitive [7, 16, 17].

Magnetic field effects on the electron beams in some studies have been considered using Monte Carlo methods. It is shown that the longitudinal non-uniform magnetic field can significantly improve electron beam dose deposition [18, 19]. It is also observed that uniform longitudinal magnetic field of 0.5 T strength can be used to reduce secondary electron out-scatter caused by the presence of an air gap, and thus improve the dose at the distal surface of air cavities [20]. The aim of this study was to verify the influence of magnetic field on the electron trajectories in order to create the desired dose distribution pattern.

2. Materials and Methods

2.1. Beam generation and dosimetry

The experiments were performed at high-energy clinac center, Ahvaz Golestan Hospital using Varian clinac 2100 C/D. 9 and 15 MeV electron beams were used in this study. Percentage depth dose (PDD) and profiles measurements were obtained using a $50 \times 50 \times 50$ cm³ water phantom (scanditronixwellhöfer, Germany), electrometer CU500 (scanditronixwellhöfer, Germany), and cylindrical ion chambers (CC13, 6186 and CC13, 6187) for field and reference dosimeter, respectively. Data analysis was undertaken using the Omni-Pro software (IBA Company). The IAEA TRS 398 dosimetry protocol was used in this study [21].

2.2. Beam shaping

The square cerrobend cutouts 4.7×4.7 cm² was made to produce 5×5 cm² field size on phantom surface (SSD=100 cm). This cutout was used in 15×15 cm² standard applicator with a gap of 5 cm to the phantom surface. The thickness of each cutout was 2 cm.

2.3. Magnetic field

The magnetic field that used in this research was produced by NdFeB permanent magnet with $60 \times 50 \times 20$ cm³ dimensions. The permanent magnets were placed around the aluminum frame on the cerrobend cutout

edge (Figure 1). These magnets were configured in 3 designs: 1) use of one magnet, 2) use of 2 parallel magnets with like poles, and 3) use of 2 parallel magnets with unlike poles. The intensity of magnetic field was measured by standard and calibrated gauss meter (BROCKHAUS Messtechnik model 410). Measurement showed that the strength of magnetic field in ion chamber site was zero so there was no concern about effect of magnetic field on ion chamber response.



Figure 1. The applicator and aluminum frame that magnet was placed on.

3. Results

Magnetic field distribution inside the frame with the permanent magnet attachment is shown in Figure 2.

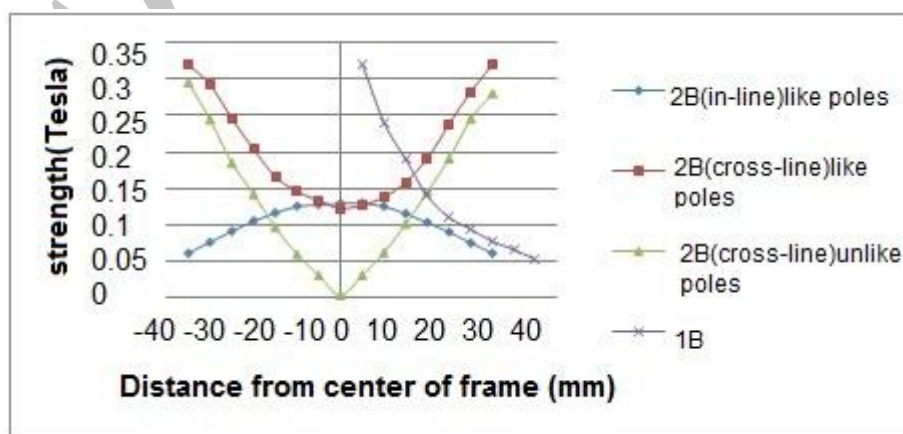


Figure 2. Magnetic field distribution for all arrangements.

When using one magnet (1B), the maximum magnetic field was measured 0.320T inside the frame and this strength decreased from the magnet toward the other side of the frame. For case of 2B (unlike poles), the maximum magnetic field at cross-line was 0.320T which decreased toward the center of the frame. This quantity at in-line was 0.129T and decreased by distance from center. For case of 2B, using unlike poles, the maximum magnetic field at cross-line was 0.296T. In this case, the magnetic field around the center of frame and at in-line direction was approximately zero.

Figures 3 and 4 show the 9 and 15 MeV electron beams central axis depth dose when the experiments arranged with and without magnetic setup. For evaluating the effect of magnetic field on dose distribution, the measurements of percentage depth dose in all situations were normalized to the maximum PDD of nonmagnetic setup. As the PDD curves demonstrate, in addition to the amount of increase in the maximum dose, the depth of this maximum was also shifted. However, the PDD measurement showed that for 15 MeV, the PDD have a rational rise and fall-off in the region before and after the d_{max} . The PDD of 9 MeV for case of 1B and 2B (like poles) in the build-up region have an unexpected behavior. However, for case of 2B (unlike poles), the d_{max} occurred in 10.2 mm with PDD = 184.8% and for this case, the PDD in buildup region have a normal rise and fall-off.

The PDD measurement showed that for all magnetic conditions, the surface dose and the dose in the buildup region were increased. This effect for 15 MeV electron beam, after applying the magnetic field demonstrated a systematic enhancement. While for the 9 MeV, electron beam surface dose enhancement in 2B (like poles) situation was less than case of 1B and 2B (unlike poles), respectively. Dose measurement in the central axis direction for 9 MeV showed noticeable event about 1B, in addition to the increase in the dose of surface and buildup region. After d_{max} , the dose reduction experienced a rapid gradient rather than the non-magnetic conditions.

In order to evaluate the effect of magnetic field on dose distribution around the central axis, the in-line and cross-line profiles in different depths were measured. Depths for 9 MeV were 20.2, 25, and 35 mm and for 15 MeV were 37, 55, and 65 mm, respectively (due to increase the number of graphs the curves for middle depth is not shown).

Profile measurement in the in-line direction for 9 MeV indicates that the magnetic field was able to increase the dose in the region near the central axis. Figure 5 shows that this increase, which coupled with the converging profile, is more considerable for two shallow depths. For greatest depth as Figure 6 shows, although the profile is still largely converged, the dose enhancement cannot occur in compare with non-magnetic condition.

Scan of in-line direction (figures 7 and 8) for 15 MeV in agreement with the 9 MeV verifies the focusing effect and dose enhancement due to application of magnetic field even for deeper depths. As can be seen in the in-line figures, for the 15 MeV electron beam, the shift of the d_{max} was not significant in comparison with 9 MeV. It should be noted that the phase difference between in-line and cross-line direction is 90 degrees. As can be seen in the cross-line measurements (Figures 9 and 10 for 9 MeV and 11 and 12 for 15 MeV) the dose distribution has lost its discipline and regularity and a tendency to lateral spread can be observed. Such conditions show the penumbra enhancement and indicate the electron being sent to areas outside of treatment field. Under 2B magnetic conditions, the 9 MeV dose deposition at depth of 20.2 and 25 mm regardless to distortion, was increased. In the two recent depths, the 1B condition increased the dose at right side and decreased the left side of cross-line profile. As shown in Figures 11, 12 although the 15 MeV cross-line profiles have been shifted to the lateral side, the less distortion is seen rather than the 9 MeV. The other remarkable note in the cross-line measurement was formation of like-wedge profile for 1B condition, while this profile for 9 MeV was formed in all three depth but for 15 MeV only at depth = 37 mm.

Effect of Magnetic Field on the PDD of Electron Beam

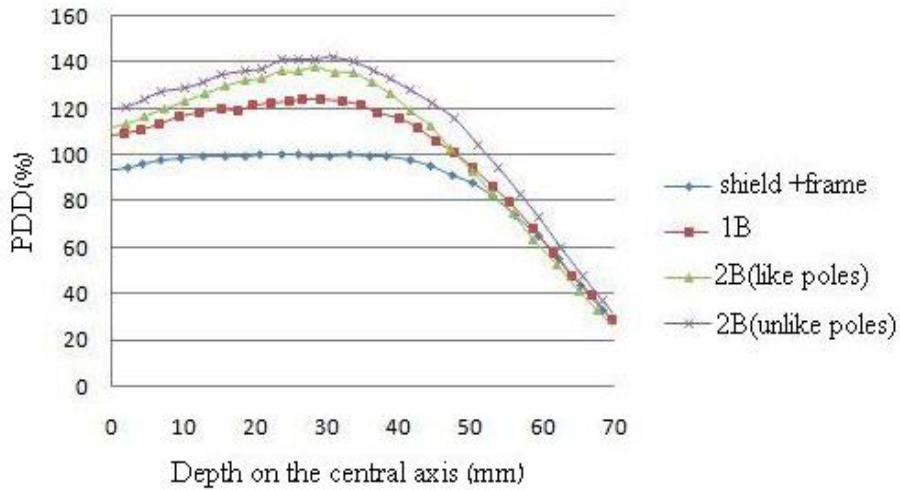


Figure 3. PDDs measurement of 15MeV electron beam for with and without magnetic setup.

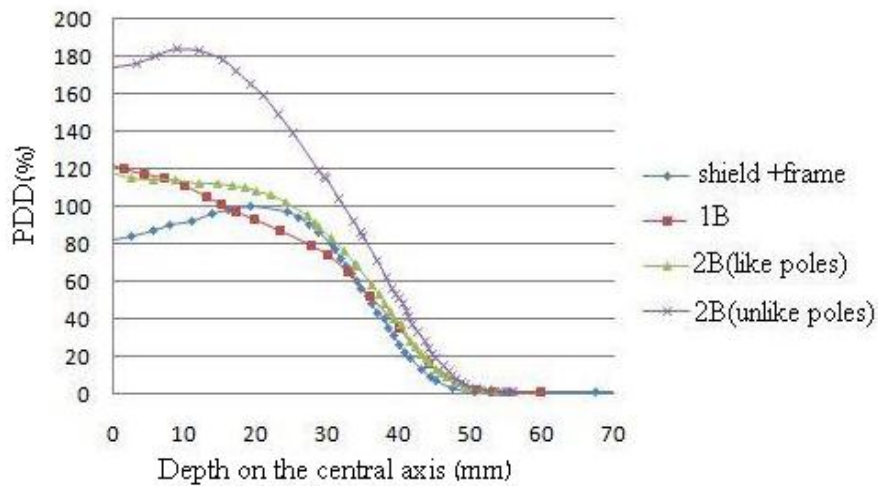


Figure 4. PDDs measurement of 9MeV electron beam for with and without magnetic setup.

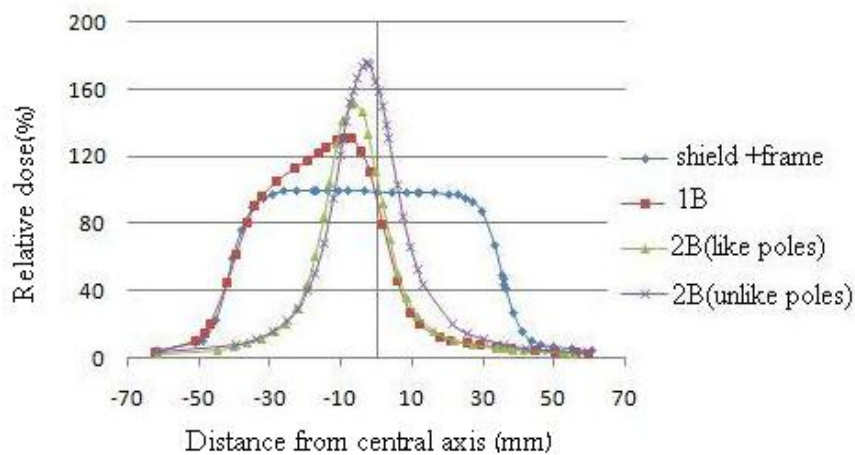


Figure 5. In-line dose distribution at depth=20.2mm for 9MeV electron beam.

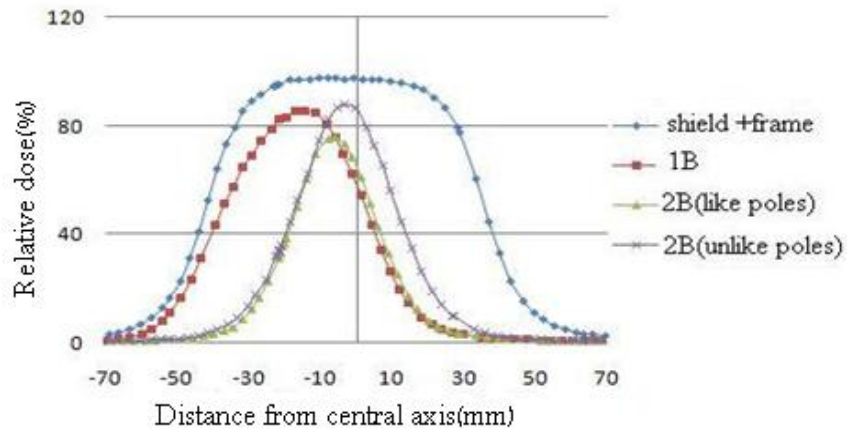


Figure 6. In-line dose distribution at depth=35mm for 9MeV electron beam.

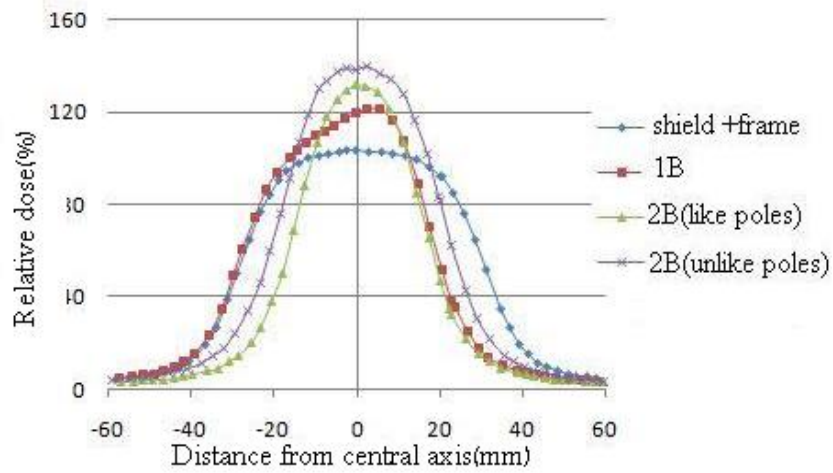


Figure 7: In-line dose distribution at depth=37mm for 15MeV electron beam.

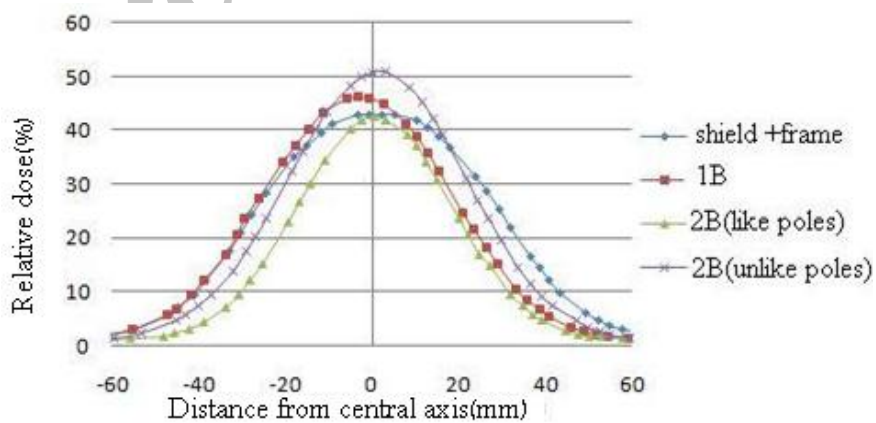


Figure 8. In-line dose distribution at depth=65mm for 15MeV electron beam.

Effect of Magnetic Field on the PDD of Electron Beam

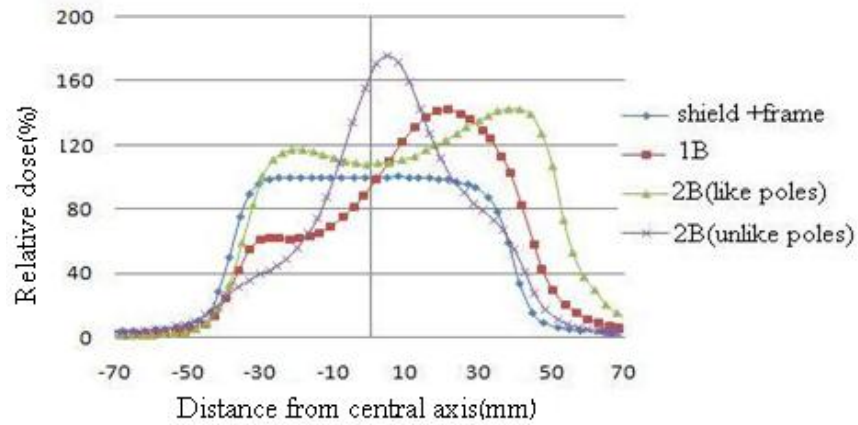


Figure 9. Cross-line dose distribution at depth=20.2mm for 9MeV electron beam.

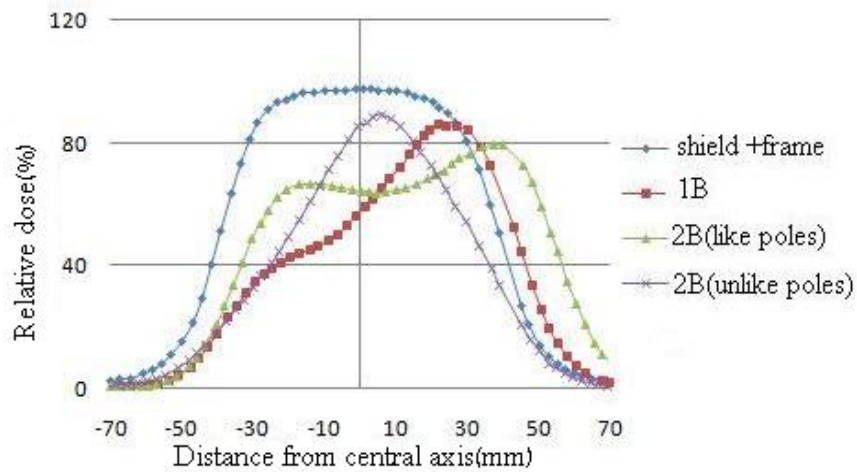


Figure 10. Cross-line dose distribution at depth=35mm for 9MeV electron beam.

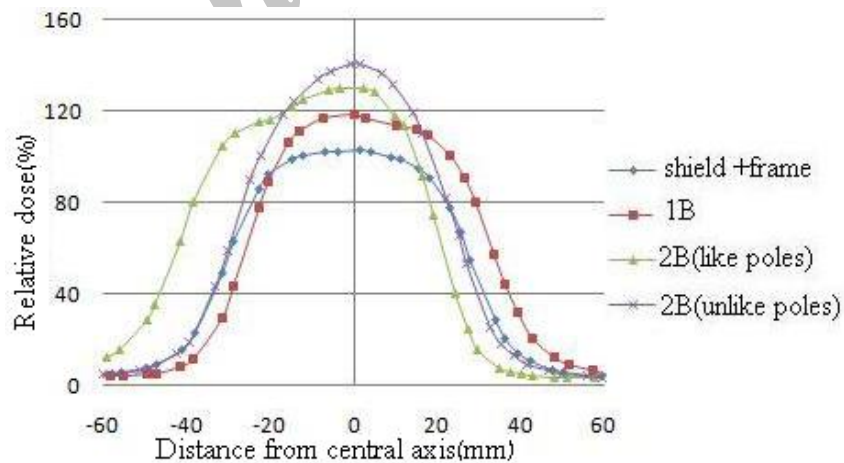


Figure 11. Cross-line dose distribution at depth=37mm for 15MeV electron beam.

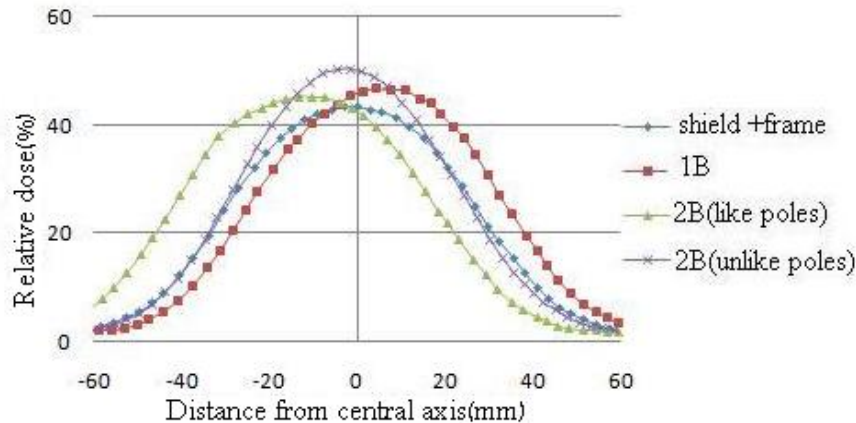


Figure 12. Cross-line dose distribution at depth=65mm for 15MeV electron beam.

4. Discussion

The PDD measurements are presented in Figures 3 and 4. Due to the collecting and focusing effect of the magnetic field, the electron flux density increased, leading to increases in the energy deposition around the central axis. From this result, it is seen that the magnetic field shifts the region of maximum dose distribution to the localized volume and this arises from the facts that a particle, which moves along a curved magnetic field line, experiences a centripetal force on its guiding path.

For 2B (unlike poles), the magnetic field near the magnets are much stronger. Because electrons can experience a more force towards the center between the poles, they are pushed and have more tendency toward the central axis. Particularly, in the energy 9MeV electrons with less velocity cause an increase in the time that it has been faced with the magnetic field. Therefore, unlike 15MeV energy, the 9MeV electrons have less opportunity to escape from the magnetic field, and as can be seen, the dose deposition in this energy represents a significant increase.

Under 1B magnetic condition, comparing the PDD curves show significant difference for both energy. As can be seen in these curves, unlike 15MeV energy, the PDD for 9MeV was reduced with linear gradient from the surface to the depth. Under this arrangement and gradient, it appears that slower electrons are not able to pass through the magnetic field. Therefore, the electrons are forced to deposit their energy in the beginning of the

path. The 40% increase in surface dose and rapid dose reduction in the build-up region confirms the argument. It should be noted that there is also such a gradient for 15MeV electron beams, but higher velocity for these electrons helps them to pass from the magnetic trap.

The angle of the particle trajectory with the vector of magnetic field is called pitch angle. When the pitch angle becomes 90 degree, the parallel component of velocity vector is reflected from lateral sides toward the center of the treatment field (This process is called mirror mechanism) [22]. It is noted that in all arrangements, the surface dose for both 9MeV and 15MeV electron beams was intensified when magnetic field was applied. The PDD measurement in Figures 2 and 3 indicate that this was due to the magnetic trapping and focusing primary electrons that reflected backward due to the mirror effect. In addition, the confinement and focusing effect of magnetic field can provide reduction of lateral scattering of the electrons.

Dosimetry in the in-line direction for both electron beams indicates, magnetic field results in a noticeable focusing of the primary electron beam, and in addition, confines the resulting dose profile. Particularly, the large penumbra generally associated with electron beams, which limits their use in radiotherapy, is significantly reduced. Magnetic in-line dose distribution compared with absence of magnetic conditions particularly increased the dose in the volume near the depth of the

maximum dose (at depth 20.2 and 25 mm for 9 MeV).

For the lower beam energy in our investigation, in-line measurement at depth of 35 mm indicates that magnetic field can return the electron beam from the deeper depth toward the surface. This could be the result of applying the mirror effect of magnetic field on the electron beam that tends to influence toward depth. Noticeable result for case of 1B in the in-line measurement is the production of wedge profile. This property as shown in the plots was more illustrious for near surface depths. Comparison between in-line measurement shows that production of wedge profile with 1B arrangement for 9 MeV was intensifier than 15 MeV electron beam. Dose profile with magnetic field produced by our 3 arrangements showed significant difference. While the 1B condition can provide confinement, it also deflects the incident electron beam, rather than focus. In contrast, the magnetic field generated by 2B conditions (both like and unlike poles) on the beam axis acts as a magnetic lens and provides both focusing properties and confinement. The focusing property can influence the electron beams parallel to the central axis and confinement feature can impress the secondary electrons that previously released their energy in the lateral border of the treatment field.

Findings of the present work is in agreement with result of some researches that used Monte Carlo methods or experimental setup particularly researches that emphasize on the dose enhancement for the region near the surface of the phantom or reduction in deeper depth. Furthermore, some researchers believe that the magnetic field can reduce the penumbra in the edge of the field size but our findings (Figures 7 and 8 for 9 MeV and Figures 11 and 12 for 15 MeV) indicate that in some areas, there is penumbra increase while there is a reduction in some other areas [15,

22, 23]. These differences could arise from differences in the selection of scan direction and attributed to the fact that increasing the dose to an area can be related to the decreasing dose in adjacent regions.

Although some researchers assert that the magnetic field can reduce surface dose [24], the most obvious finding to emerge from the present study was that the magnetic field can increase the surface dose for all their arrangements. These differences can be caused by the strength and type (e.g., longitudinal, transverse, complex) of magnetic field or revert to region that the magnetic field is applied. This explanation does not include photon beams. As showed in other studies, the reduction of surface dose in photon beams encounter to magnetic field is due to the elimination of electron contamination [25, 26].

5. Conclusion

NdFeB rare earth permanent magnets can produce strong magnetic field restricted to small area with a rapid fall-off. Our finding shows that use of magnetic field can change the dose-deposition patterns, so by this effect can produce dose enhancement as well as dose reduction in localized regions for high-energy electron beams. The locations of these high- and low-dose regions are potentially adjustable to enhance the dose to the target volume and decrease the dose to normal tissues in radiation therapy.

Acknowledgment

This research was supported by a grant from Ahvaz Jundishapur University of Medical Sciences (u-90085). This work was done in Department of Radiation Oncology of Ahvaz Golestan Hospital, and the authors would like to thank the members of this department for their valuable assistance.

References

1. Halliday D, Resnick R, Walker J. Fundamentals of physics extended. Wiley.com; 2010.

2. Reitz JR, Milford FJ, Christy RW. Foundations of electromagnetic theory. Addison-Wesley Publishing Company; 2008.
3. Lazarakis P, Bug MU, Gargioni E, Guatelli S, Incerti S, Rabus H, et al. Effect of a static magnetic field on nanodosimetric quantities in a DNA volume. *International journal of radiation biology*. 2012 Jan;88(1-2):183-8.
4. Raylman RR, Clavo AC, Wahl RL. Exposure to strong static magnetic field slows the growth of human cancer cells in vitro. *Bioelectromagnetics*. 1996;17(5):358-63.
5. Bostick WH. Possible techniques in direct-electron beam tumor therapy. *Phys Rev*. 1950;77:564-5.
6. St Aubin J, Steciw S, Fallone BG. Effect of transverse magnetic fields on a simulated in-line 6 MV linac. *Physics in medicine and biology*. 2010 Aug 21;55(16):4861-9.
7. Nettelbeck H, Takacs GJ, Rosenfeld AB. Effect of transverse magnetic fields on dose distribution and RBE of photon beams: comparing PENELOPE and EGS4 Monte Carlo codes. *Physics in medicine and biology*. 2008 Sep 21;53(18):5123-37.
8. Raaijmakers AJ, Raaymakers BW, van der Meer S, Lagendijk JJ. Integrating a MRI scanner with a 6 MV radiotherapy accelerator: impact of the surface orientation on the entrance and exit dose due to the transverse magnetic field. *Physics in medicine and biology*. 2007 Feb 21;52(4):929-39.
9. Shih CC. High energy electron radiotherapy in a magnetic field. *Medical physics*. 1975 Jan-Feb;2(1):9-13.
10. Sempert M. New developments in high energy electron beam therapy with the 35 MeV Brown Boveri betatron. *Radiology*. 1960 Jan;74:105-6.
11. Chu JC, Reiffel L, Hsi WC, Saxena VA. Modulation of radiotherapy photon beam intensity using magnetic field. *International journal of cancer Journal international du cancer*. 2001;96 Suppl:131-7.
12. Chu JC, Reiffel L, Li XA, Hsi W, Naqvi S, Ye S, et al. Tumor dose enhancement and normal tissue protection using magnetic field modulated photon beams in radiation therapy. *International Journal of Radiation Oncology*Biophysics*Physics*. 2000;48(3, Supplement 1):338.
13. Litzenberg DW, Fraass BA, McShan DL, O'Donnell TW, Roberts DA, Becchetti FD, et al. Experimental apparatus to measure the effect of strong longitudinal magnetic fields on photon and electron radiotherapy beams. *Phys Med Biol*. 2001;46:N105.
14. Litzenberg DW, Fraass BA, McShan DL, O'Donnell TW, Roberts DA, Becchetti FD, et al. An apparatus for applying strong longitudinal magnetic fields to clinical photon and electron beams. *Physics in medicine and biology*. 2001;46(5):N105.
15. Chen Y, Bielajew AF, Litzenberg DW, Moran JM, Becchetti FD. Magnetic confinement of electron and photon radiotherapy dose: a Monte Carlo simulation with a nonuniform longitudinal magnetic field. *Medical physics*. 2005 Dec;32(12):3810-8.
16. Belousov A, Varzar' S, Chernyaev A. Simulation of the conditions of photon and electron beam irradiation in magnetic fields for increasing conformity of radiation therapy. *Bulletin of the Russian Academy of Sciences: Physics*. 2007;71(6):841-3.
17. Kirkby C, Stanescu T, Fallone BG. Magnetic field effects on the energy deposition spectra of MV photon radiation. *Physics in medicine and biology*. 2009 Jan 21;54(2):243-57.
18. Oborn B, Metcalfe P, Butson M, Rosenfeld AB, Keall P. Electron contamination modeling and skin dose in 6 MV longitudinal field MRIgRT: Impact of the MRI and MRI fringe field. *Medical physics*. 2012;39:874.
19. Belousov AV, Plotnikov AB, Chernyaev AP, Shvedunov VI. Increasing the Efficiency of Target Irradiation with Photon and Electron Beams in Radiation Therapy. *Instruments and Experimental Techniques*. 2003;46(6):828-31.
20. Jackson JD, Fox RF. Classical electrodynamics. *American Journal of Physics*. 1999;67:841.
21. IAEA. Absorbed Dose Determination in Electron Beam Radiotherapy: An International Code of Practice for Dosimetry Based on Standards of Absorbed Dose to Water IAEA Technical Report Series No 398. 2004.
22. Becchetti FD, Litzenberg DW, Moran JM, O'Donnell TW, Roberts DA, Fraass BA, et al. Magnetic confinement of radiotherapy beam-dose profiles. *AIP Conf Proc*. 2001 Dec 12;600(1):44-6.
23. Bielajew AF. The effect of strong longitudinal magnetic fields on dose deposition from electron and photon beams. *Medical physics*. 1993 Jul-Aug;20(4):1171-9.
24. Saberi H, Bahreyni Toosi M. T. The Study of Magnetic Field Effects on the Electron Contamination of Neptun 10 PC. *Iran Jour Med Phys*. 2007;3(13):31-40.
25. Butson M, Yu P, Kan M, Carolan M, Young E, Mathur J, et al. Skin dose reduction by a clinically viable magnetic deflector. *Australasian physical & engineering sciences in medicine/supported by the Australasian College of Physical Scientists in Medicine and the Australasian Association of Physical Sciences in Medicine*. 1997;20(2):107.
26. Butson MJ, Cheung T, Yu P, Metcalfe PE. Evaluation of a radiotherapy electron contamination deflecting system. *Radiation Measurements*. 2000;32(2):101-4.

Surf and download all data from SID.ir: www.SID.ir

Translate via STRS.ir: www.STRS.ir

Follow our scientific posts via our Blog: www.sid.ir/blog

Use our educational service (Courses, Workshops, Videos and etc.) via Workshop: www.sid.ir/workshop